An Online Data-Driven Technique for the Detection of Transformer Winding Deformations

Tianqi Hong, *Student Member, IEEE*, Digvijay Deswal, *Student Member, IEEE*, and Francisco de León, *Fellow, IEEE*

***Abstract*—This paper presents a novel online diagnostics method capable of detecting winding deformations in two-winding single-phase transformers. The main idea is to identify changes in the short-circuit impedance. The combination of 3-D Lissajous curve methods with a Butterworth low-pass filter allows for the accurate determination of winding deformation of large power transformers in real time. The method is very robust and capable of detecting deformations at the early stage even when the measurements are noisy. Only information already available to the differential protection relay is needed. The proposed diagnostics method has been validated with circuit and finite element simulations plus a lab experiment. Results show that the proposed online diagnostics technique has the ability to identify winding deformation problems under severe conditions, such as non-sinusoidal input, nonlinear loading, and measurement noise. Under ideal conditions (no signal noise), the inductive identification error of the proposed online diagnostics method identifies the parameters with less than 0.09% error. When accepting measurement noise of 1%, the error on the identification of inductance is less than 0.13%.**

***Index Terms*— Lissajous curve methods, measurement noise, non-sinusoidal excitation, nonlinear loading, two-winding single-phase transformers, winding deformation detection.**

I. Introduction

GRID modernization is a major task in today's power industries. Implementing smart technologies in power systems is a prime objective. Apart from smart power electronics equipment, monitoring and detection systems for already installed equipment should be updated. Transformers are critical components of power systems. Consequently, the monitoring and protection systems for modern transformers play key roles in the improvement of their reliability and as a consequence that of modern power systems.

Transformer windings are subjected to strong electromagnetic forces when faults occur. The electromagnetic force increases with the short circuit current level. As time passes and a transformer endures large short-circuit currents, its windings gradually deform. Once the windings start to deform, the damage accumulates. To avoid crucial damage, it is necessary to detect the winding deformation at an early stage.

There exist various reliable offline test methods, such as the Frequency-Response Analysis (FRA), the Short Circuit Impedance Analysis (SCIA), and the Low Voltage Impulse (LVI) test [1]-[4]. Offline tests provide full freedom to perform reliable condition testing. Among the offline detection methods, FRA is the most used since it is able to identify both electrical and mechanical abnormalities of a transformer accurately [4]-[6]. However, it is impractical to take a transformer offline frequently. This is particularly true for transformers of large capacities. Thus the aim to develop online diagnostics techniques has sprouted out recently.

In the past decades, a variety of online diagnostics methods have been proposed. The majority of those methods can be seen as extensions of offline diagnostics methods [4]. Since FRA is more accurate and reliable than the other detection methods, online FRA methods have been proposed in [6]-[9]. According to [6]-[9], the healthy data of the transformer, extra high-frequency signal generator, and linear loading condition are three key factors for successfully implementing online FRA in the field.

Although the online FRA methods have higher accuracy than online SCI methods, the capital investment of online SCI methods is less than that of online FRA. Hence, several online SCI methods are proposed for solving the transformer deformation or inner fault detection problems [10]-[11]. A novel 2-D Lissajous curve (2DLC) method is proposed in [10]. This is the first paper that links the Lissajous curve method with transformer winding abnormality detection. The relationship between the short circuit impedance of a transformer and the winding abnormality has been validated by simulation and experimental studies.

With the development of modern power grids, the loads in power systems become nonlinear. Correspondingly, the input voltage may not be a pure fundamental sine wave. In [11], an online diagnostics method considering the impact of voltage harmonics has been proposed. The method is another application of the 2DLC method. However, 2DLC method is only a part of the complete Lissajous curve method. Useful information hidden in the terminal measurements is not fully utilized for identification [12].

A practical and implementable online diagnostics method should consider nonlinear loading conditions and input voltage distortion. Additionally, the impacts from measurement noise are important for practical implementations. In this paper, a novel data-driven online diagnostics technique based on the 3-D Lissajous curve (3DLC) method [12] is proposed for

The authors are with the Department of Electrical and Computer Engineering at New York University, Five Metro-tech Center, Brooklyn, NY, 11201 (e-mails: th1275@nyu.edu, dd1681@nyu.edu, fdeleon@nyu.edu).

transformer winding deformation detection. Since the 3DLC is a more powerful graphical tool which utilizes more information from the terminal measurements, the deformation detection method is robust even under very severe conditions (variable load, non-sinusoidal excitation, and noisy measurements). The proposed method is an application and improvement of the 3-D Lissajous method described in [12]. Several simulation studies are provided in this paper to validate the advantages and accuracy of the proposed method for the detection of winding deformation or abnormality.

The scope of this paper is to detect deformations and abnormalities (on-line) of two-winding single-phase transformers operating under normal conditions. The purpose of the method is to send an alarm to the operator indicating that the transformer needs to be examined to prevent severe damage. The method is not aimed at sending disconnecting signals to the protective relays to take the transformer off-line instantly. Reliability over detection speed is favored to prevent false positives.

II. Theoretical Considerations of Transformer Winding Deformation Diagnostics

Theoretically, the short-circuit impedance is an indicator of transformer winding deformations. Hence, the proposed method is in essence an online leakage impendence identification process. It is worth to point out that this paper does not focus on investigating the relationships between winding deformation types and the impact on the change of the short circuit impedance.

To measure the short-circuit impedance online, we start by analyzing the steady state model of a transformer. In the literature, there are two transformer equivalent circuit models: the classic T model and the π model. The structures of those two models are shown in Figs. 1(a) and (b). The proposed online diagnostics approach is obtained from the analysis of the T equivalent circuit and validated with the π equivalent and finite element models in Sections III and IV. In the following discussion, we assume that all electrical parameters are referred to the primary side of a transformer.

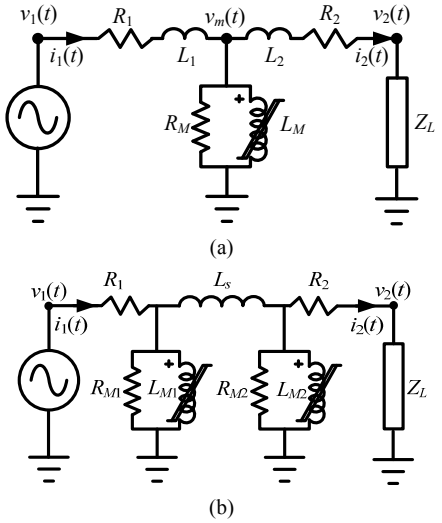

Fig. 1. Two equivalent circuits for a transformer: (a) T equivalent circuit; (b) π equivalent circuit.

A. Theoretical Background

From the T equivalent circuit of a transformer shown in Fig. 1(a), we can obtain:

$$v_1(t) - v_m(t) = R_1 i_1(t) + L_1 \frac{d}{dt} i_1(t) \tag{1}$$

$$v_m(t) - v_2(t) = R_2 i_2(t) + L_2 \frac{d}{dt} i_2(t) \tag{2}$$

where $v_1(t)$ and $i_1(t)$ are the instantaneous voltage and current of primary side; $v_2(t)$ and $i_2(t)$ are the instantaneous voltage and current of secondary side; R_1 and L_1 are the equivalent winding resistance and leakage inductance of primary; R_2 and L_2 are the equivalent winding resistance and leakage inductance of secondary; $v_m(t)$ is the voltage of the magnetizing branch (representing the core flux). $v_m(t)$ does not exist physically, but is very useful for analysis.

For the purpose derivations only, we assume that $R_1 = R_2 = 0.5\,R_T$ and $L_1 = L_2 = 0.5\,L_T$. The assumption is not a requirement for the implementation of the identification method; see Section III for more details. From (1) and (2), we have:

$$\begin{aligned} v_{12}(t) &= v_1(t) - v_2(t) \\ &= \frac{R_T}{2}[i_1(t) + i_2(t)] + \frac{L_T}{2}\frac{d}{dt}[i_1(t) + i_2(t)] \\ &= \frac{R_T}{2} i_{12}(t) + \frac{L_T}{2}\frac{d}{dt} i_{12}(t) \end{aligned} \tag{3}$$

where $v_{12}(t)$ is the voltage across the leakage impedance, $i_{12}(t)$ is the sum of $i_1(t)$ and $i_2(t)$. Using the theory presented in [12] we can plot the 3-D Lissajous curve with axes $i(t)$, $\mathrm{d}i(t)/\mathrm{d}t$ and $v(t)$ of (3). An example Lissajous curve for a 300 MVA transformer is plotted in Fig. 2. One can easily find that the 3-D Lissajous curve is located in plane A. The parameters R_T and L_T describing plane A can be computed using three measurement points (say points a_1, a_2, and a_3 in Fig. 2).

We note that the 3-D Lissajous curve method proposed in [12] is sensitive to measurement noise. To improve its robustness, additional measurements are collected and the plane identification problem is converted into an optimization problem.

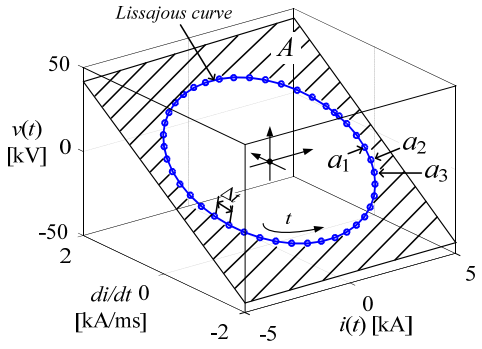

Fig. 2. 3-D Lissajous curve for a 300 MVA transformer.

To illustrate the data-driven online diagnostics process, we start with the discussion of the discretized data acquisition system. The sampling frequency is f_s and the corresponding

sampling time is Δt. The k^{th} data set obtained from the acquisition system is denoted as $\{v_{12}[k], i_{12}[k]\}$, where $v_{12}[k]$, $i_{12}[k]$ are discretized $v_{12}(t)$ and $i_{12}(t)$ of the k^{th} sample. Each data set satisfies (3). After N data sets are collected, we have:

$$\begin{bmatrix} v_{12}[1] \\ \vdots \\ v_{12}[N] \end{bmatrix} = \begin{bmatrix} i_{12}[1] & \left.\frac{d}{dt} i_{12}(t)\right|_{t=\Delta t+t_0} \\ \vdots & \vdots \\ i_{12}[N] & \left.\frac{d}{dt} i_{12}(t)\right|_{t=N\Delta t+t_0} \end{bmatrix} \begin{bmatrix} \frac{R_T}{2} \\ \frac{L_T}{2} \end{bmatrix} \tag{4}$$

where N is the observation window length; t_0 is the initial time and assumed to be zero in this paper. When the measurements are sufficiently accurate, the current derivative can be approximated by a first-order difference to save computational power. Yielding:

$$\left.\frac{d}{dt} i_{12}(t)\right|_{t=k\Delta t} = \frac{i_{12}[k+1] - i_{12}[k]}{\Delta t} \tag{5}$$

For simplicity, we convert (4) into a matrix as follows:

$$\boldsymbol{V}_{12} = \frac{1}{2}\boldsymbol{I}_{12}\begin{bmatrix} R_T \\ L_T \end{bmatrix} \tag{6}$$

where $\boldsymbol{V}_{12}$ is a $N \times 1$ column vector containing the information of instantaneous voltage measurements; $\boldsymbol{I}_{12}$ is a $N \times 2$ matrix containing the information of instantaneous current measurements and its derivative. By minimizing the 2-norm of the difference between the left and right sides of (6), we obtain:

$$\begin{bmatrix} R_T \\ L_T \end{bmatrix} = \arg\min_{R_T, L_T} \left\| \boldsymbol{V}_{12} - \frac{1}{2}\boldsymbol{I}_{12}\begin{bmatrix} R_T \\ L_T \end{bmatrix} \right\|_2 \tag{7}$$

Solving problem (7) as a standard ridge regression, the following analytical solution is obtained [13]:

$$\begin{bmatrix} R_T \\ L_T \end{bmatrix} = 2(\boldsymbol{I}_{12}^T\boldsymbol{I}_{12} + \lambda\boldsymbol{E})^{-1}\boldsymbol{I}_{12}^T\boldsymbol{V}_{12} \tag{8}$$

where λ is a regulation factor used in cases when $\boldsymbol{I}_{12}^T\boldsymbol{I}_{12}$ is ill-conditioned; $\boldsymbol{E}$ is the identity matrix of the same dimension as $\boldsymbol{I}_{12}^T\boldsymbol{I}_{12}$. Based on our experience, $\boldsymbol{I}_{12}^T\boldsymbol{I}_{12}$ normally has an acceptable condition number. Hence, λ is set to zero for most cases. Under the extreme situation when the condition number of $\boldsymbol{I}_{12}^T\boldsymbol{I}_{12}$ is larger than 10^5, λ is set to 0.01. Based on our experience this solves all problems with ill-conditioned matrices.

Note that (8) is a very simple equation which can be calculated directly based only on online measurements regardless the shapes of voltage and current waveforms. Different from most of the previous studies, the proposed online diagnostics method has no strict requirements on the quality of the input voltage and the load connected to the transformer.

B. Application to Transformer Diagnostics

According to the IEEE Std. 62 [14], changes in total winding resistance within 5% are considered satisfactory. This means that the maximum allowable deviation of the winding resistance is 5%. Meanwhile, the maximum allowable deviation of the leakage inductance is 3% [14]. As a result, the error of the online diagnosis process should be much smaller than 3% for leakage inductance and 5% for winding resistance. Hence, numerical errors are critical especially when the deformation has just occured (minor change in the short-circuit impedance).

The leakage impedance (inductance) of large power transformers is usually much larger than the winding resistance. Therefore, it is crucial to compute the derivatives of the current accurately. When the measurements are not accurate (have noise), the inaccuracies will be magnified by taking derivatives. According to (5), the standard deviation of the error introduced by white noise will be amplified by $\sqrt{2}/\Delta t$ times. Hence, merely increasing the sampling rate f_s (using a faster data acquisition system) will reduce the numerical measurement error, but magnify the error introduced by noise.

Using a high order differentiation method is a sensible choice to solve the problem. An 8-point stencil central differences (SCD) method is applied in this paper to reduce the effect of noise. The mathematical expression of the 8-point SCD method at the k^{th} sample is [15]:

$$\begin{aligned} \left.\frac{d}{dt} i\right|_{t=k\Delta t} \approx & \frac{4(i_{k+1} - i_{k-1})}{5\Delta t} - \frac{(i_{k+2} - i_{k-2})}{5\Delta t} \\ & + \frac{4(i_{k+3} - i_{k-3})}{105\Delta t} - \frac{(i_{k+4} - i_{k-4})}{280\Delta t} \end{aligned} \tag{9}$$

where i is the target current function; the subscript is the sample index. To calculate the initial derivative of the current, the current measurement from previous observation window can be used.

C. De-Noising Implementation

Measurement noise is a nuisance for all online diagnostics methods. As mentioned before, the noise is amplified when taking the derivatives during the numerical computation process. To minimize the impact from measurement noise, it is better to select a larger observation window length N at the cost of a slower response time to the system dynamics.

The winding deformation monitor is a system for protecting transformers in steady state. Hence, the dynamic performance can be sacrificed a little to improve accuracy and robustness to measurement noise. The relationship between sampling frequency f_s and the observation window length N is:

$$N = \alpha \cdot N_c = \alpha \cdot \frac{f_s}{f_1} \tag{10}$$

where N_c is the number of the samples per cycle and f_1 is the fundamental frequency of the target power system; α is a positive integer. According to (10), the diagnostics system performs leakage impedance identification every α cycles.

Instead of selecting a large observation window length N, a low-pass filter has been attached after the identification process. The transfer function of a digital Butterworth low-pass filter of m-order can be expressed as:

$$H(z) = \frac{\mathrm{Y}(z)}{X(z)} = \frac{b(1) + b(2)z^{-1} + \cdots + b(m+1)z^{-m}}{a(1) + a(2)z^{-1} + \cdots + a(m+1)z^{-m}} \tag{11}$$

where $a(k)$ and $b(k)$ are the transfer function coefficients which can be obtained from the cutoff frequency of the low-pass filter [16]. According to (11), the output of the low-pass filter at the $(k+1)^{th}$ sample is:

$$y[k+1] = b(1)x[k+1] + r_1[k] \tag{12}$$

where

$$r_i[k] = b(i+1)x[k] + r_{i+1}[k-1] - a(i+1)y[k],$$
$$r_m[k] = b(m+1)x[k] - a(m+1),$$

$x[k+1]$, $y[k+1]$ are the input and output of the low-pass filter at

the $(k+1)^{th}$ time step; $r_i[k]$ has the information of the past, which can be used to set the output initial value of the low-pass filter.

In this paper, the input and output of the low-pass filter are the total winding resistance or total leakage inductance obtained from (8). The initial values of the low-pass filter are set to be the leakage impedance obtained from the factory impedance test. The initial value of the winding resistance needs to be constantly adjusted because it changes with temperature. The IEEE Std. 62 [14] gives the following expression:

$$R_T[0] = R_{T,t_0}\frac{T_t + T_{copper}}{T_{t0} + T_{copper}} \tag{13}$$

where $R_T[0]$ is the initial value of the winding resistance to be entered to the low-pass filter, T_t is the temperature at which the resistance was measured in ˚C, T_{t0} is the reference temperature in ˚C, R_{T,t_0} is the winding resistance measured at T_{t0}; T_{copper} is a constant equals to 234.5˚C for copper windings. If temperature measurements are not available, the winding resistance cannot be used as an indicator for winding deformation and one must rely only on the changes in inductance. In the following discussion, we assume that temperature measurements are available and the initial value of the winding resistance has been adjusted accordingly. The flow chart of the proposed online diagnostics method is shown in Fig. 3.

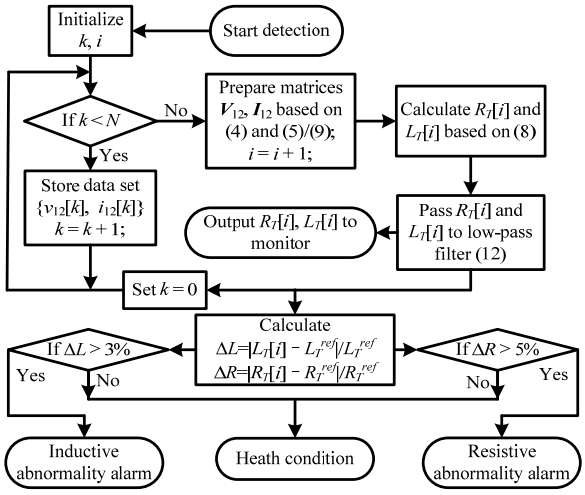

Fig. 3. Flowchart of the transformer winding diagnostics process.

D. Discussion of Assumptions

Most of the existing online SCI methods assume that the input voltage is sinusoidal and the load connected to the transformer is linear. In comparison, the proposed method has no requirements on the input voltage or load behavior. However, several assumptions were made during the derivation of the proposed online diagnostics method. We assumed that a transformer could be modeled by a *T* equivalent circuit with identical equivalent winding resistance and leakage inductance of the primary and secondary windings. The *T* equivalent circuit is not the best choice for modeling single phase transformers in the presence of saturation [17]. Additionally, winding resistances of primary and secondary depend on the wire gauge, the number of turns, winding dimensions, manufacturing process, etc.

The assumptions mentioned above are not strict requirements for the implementation of the proposed method. In the following section, the winding resistance and leakage inductance are distributed in a realistic fashion, meaning $R_1 \neq R_2$ and $L_1 \neq L_2$. A hysteretic inductor represents the core (nonlinear magnetizing current and losses) in the simulation studies. The simulations are made as realistic as possible.

III. Numerical Example with Transformer Equivalent Model

Sinusoidal voltage excitation and supplying linear loads are the expected working conditions of a transformer. However, loads are increasingly becoming more nonlinear because of the widespread use of power electronics supplies. To validate the accuracy and robustness of the proposed online diagnostics method, several numerical examples are provided in this section.

A. Evaluation of the Identification Error using Simulated Terminal Data from Different Transformer Models

Based on the simulated measurement data, the proposed diagnostics method is applied to identify the short-circuit impedances when the transformer is loaded at rated condition.

The equivalent circuits of *T* and π models shown in Fig. 1 are built in EMTP-RV [18]. The corresponding circuit parameters of the *T* and π models are listed in Table I. All the parameters are obtained from a real 300 MVA transformer from [19] and referred to the primary side. The medium voltage winding is not used in this study. The magnetizing inductances are modeled using hysteresis curves.

TABLE I
Circuit Parameters for *T* and π Circuits

R_1 [Ω]	R_2 [Ω]	L_{s1} [mH]	L_{s2} [mH]	R_m [kΩ]	L_s [mH]	R_{m1}, R_{m2} [kΩ]
0.26	0.2605	15.1	20	53	35.1	106

The voltage sources for the two circuits are cosine functions:

$$v(t) = V_m \cos(\omega_1 t) \tag{14}$$

where V_m equals to 281.7 kV and ω_1 equals to 120π. The simulation time step is 20 μs. The sampling frequency of the data acquisition system is 2.5 kHz which means 50 data points per cycle. Several commercial transformer monitors or digital differential relays claim that they can provide faster sampling frequencies [20]-[21]. Hence, additional investment in data acquisition systems is not needed for the proposed method. The rated load with unity power factor is connected to the two transformer models, namely Z_L = 131.92 [Ω].

The maximum identification error in percent between the identified R_T and its reference is calculated as:

$$\Delta\overline{R_T} = \frac{\max\left|R_T(t) - R_T^f\right|}{R_T^f} \times 100\% \tag{15}$$

where $\Delta\overline{R_T}$ is the maximum identification error in percent; R_T^f is the reference winding resistance obtained from the impedance test (and considering variations with temperature). The maximum identification error of leakage inductance $\Delta\overline{L_T}$ is calculated in a similar manner.

The time sequence identification errors are shown in Fig. 4.

The maximum identification errors on the winding resistance and leakage inductance are summarized in Table II. According to the results shown in Table II, the maximum error in total winding resistance R_T is 0.196% and the maximum error in leakage inductance L_T is only 0.074%. The error in the identification process comes from the computation process of derivatives and nonlinear currents from the nonlinear magnetizing branches.

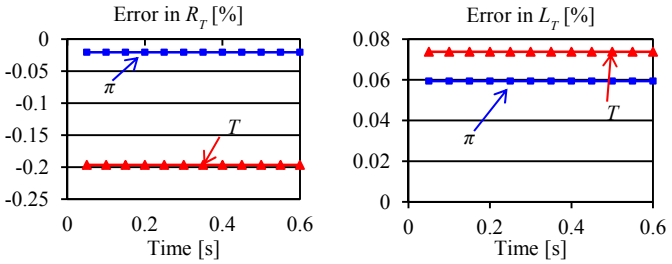

Fig. 4. Identification errors when using simulated terminal measurements: (a) Identification error in total winding resistance R_T (0.5206 Ω); (b) Identification error in total leakage inductance L_T (35.1 mH).

TABLE II
MAXIMUM ERROR IN PERCENT UNDER RATED LOADING

	$\Delta\overline{R_T}$ [%]	$\Delta\overline{L_T}$ [%]
T model	0.196	0.074
π model	0.020	0.059

Comparing $\Delta\overline{R_T}$ and $\Delta\overline{L_T}$, one can appreciate that the identification error is not equally distributed between R_T and L_T since $\omega_1 L_T$ is much larger than R_T; see Table I. This phenomenon brings significant problems to the identification of the winding resistance when measurement noise is considered. For now, the identification results of the leakage impedance with the two models are small and acceptable. According to Fig. 4, the identification results of T and π models are close to each other. The maximum deviation of the identification results between T and π models is 0.18%. Although the derivation of (8) is obtained using the T equivalent circuit, the identification accuracy is higher when the π equivalent circuit is used to simulate transformer terminal measurements. According to [17] and [22], the π model is more accurate than the T model for the representation of transformers. Hence, the π model is used to simulate the transformer terminal measurements in the next four numerical studies.

B. Evaluation of the Identification Error when Changing Loading

The load is modeled as constant impedance during at least one fundamental period in this example. Changes in the loading conditions are defined as changes in the amplitude of the current and power factor. Without magnetizing branch, the identification process is independent of the changes in the loading conditions. However, the magnetizing branch current cannot be neglected in practice. In this subsection, the impacts coming from the loading condition are discussed in detail.

In the following examples, several loading scenarios are simulated with the π equivalent circuit. The loading conditions are summarized in Table III. For a normal power system, the power factor is commonly larger than 0.8. Hence, both the normal operation (power factor = 0.985) and the worst condition (power factor = 0.707) are considered.

When the transformer is loaded at rated current, the accuracy of the identification results is affected by the changes in power factor; see Fig. 5. The maximum identification errors from cases 1 to 8 are summarized in Table IV. Accordingly, the identification error of the winding resistance is larger when a capacitive load is connected to the transformer. In contrast, the maximum inductive identification error occurs when the transformer is loaded by a lightly inductive load. Although $\Delta\overline{R_T}$ is almost 5 times larger than $\Delta\overline{L_T}$ (see Table IV), the simulation results show that the proposed method still can be used for identifying transformer winding deformations.

TABLE III
LINEAR LOADING CONDITIONS (*RLC* IN SERIES)

	$\lvert Z_L\rvert$ [Ω]	R_L [Ω]	L_L [mH]	C_L [μF]	Power Factor
Case 1	131.92 (rated)	131.92	0	0	1
Case 2		129.92	60.76	0	0.985 (lagging)
Case 3		93.28	247.4	0	0.707 (lagging)
Case 4		93.28	0	28.4	0.707 (leading)
Case 5		129.92	0	115.8	0.985 (leading)
Case 6	263.84 (half)	263.84	0	0	1
Case 7		186.56	494.87	0	0.707 (lagging)
Case 8		186.56	0	14.2	0.707 (leading)

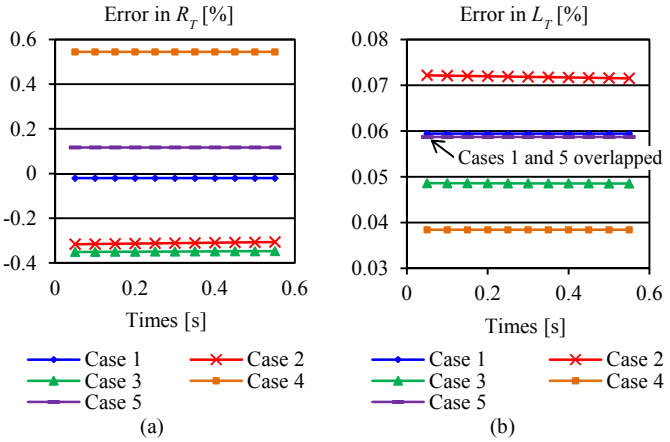

Fig. 5. Identification errors for a fully loaded transformer. (a) Identification errors in R_T (0.5206 Ω) from cases 1 to 5; (b) Identification errors in L_T (35.1 mH) from cases 1 to 5.

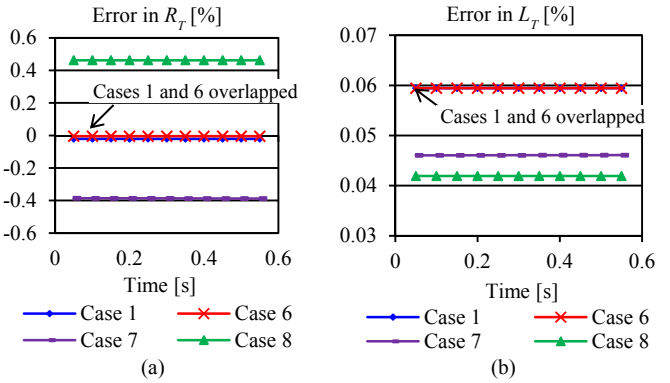

Fig. 6. Identification errors for a half loaded transformer. (a) Identification errors in R_T (0.5206 Ω) from cases 1 and 6 to 8; (b) Identification errors in L_T (35.1 mH) from cases 1 and 6 to 8.

TABLE IV
MAXIMUM DIFFERENCES IN PERCENT FOR CASES 1 TO 8

Case	1	2	3	4	5	6	7	8
$\Delta\overline{R_T}$ [%]	0.02	0.32	0.35	0.55	0.12	0.00	0.39	0.46
$\Delta\overline{L_T}$ [%]	0.06	0.07	0.05	0.04	0.06	0.06	0.05	0.04

When the transformer is supplying half load, the maximum identification errors of the total leakage inductance and the total winding resistance do not change significantly. Comparing with Figs. 5 and 6, we conclude that the impact of the power factor is larger than the impact of the amplitude of the current. It worth to point out that the impact of the loading level becomes dominant when the transformer is lightly loaded. The maximum identification error will rise to 3% on winding resistance and 2.4% on leakage inductance when the transformer is loading at 20% of the rated capacity. Hence, to detect winding deformation one needs to have a significant current flowing in the windings (much larger than the magnetizing and capacitive currents), situation that will happen during a typical day in the normal operation of a transformer.

C. Evaluation of the Identification Error Considering Measurement Noise

In practice, all measurements are imperfect. Noise can pollute the measurements and introduce errors to the diagnostics method. In all the following examples measurement noise is considered. The settings for Cases *A* to *F* are summarized in Table V. In this study, Case *A* corresponding to the worst case scenario (half loaded with 0.707 leading power factor) is simulated with noise to evaluate the robustness of the proposed method.

TABLE V
EXAMPLE SETTINGS FROM CASES A TO F

	Loading Condition	Change [%]		Noise [%]	Digital filter	
		R_T	L_T		Order	Cutoff
Case A	Case 8	0	0	1	3	25 Hz
Case B	Case 8	5	3	1	3	25 Hz
Case C	Case 8	-5	-3	1	3	25 Hz
Case D	Case 8	5	3	1	5	5 Hz
Case E	Case 8	5	-5	1	3	25 Hz
Case F	Fig. 9(b)	5	-5	1	3	25 Hz

To simulate noisy measurements, white noise is added to the measurements as follows:

$$v_i'[k] = v_i[k] + \tilde{\alpha}_i \quad i = 1,2$$
$$i_i'[k] = i_i[k] + \tilde{\beta}_i \quad i = 1,2 \tag{16}$$

and

$$\tilde{\alpha}_i \sim \mathcal{N}(0, \sigma_v^2) \qquad \tilde{\beta}_i \sim \mathcal{N}(0, \sigma_i^2)$$

where $v_i'[k]$ and $i_i'[k]$ are the k^{th} voltage and current with noise; σ_v and σ_i are the standard deviations of the noise added to voltage and current, respectively. In the following examples, $3\sigma_v$ is set to 1% of the amplitude of the primary voltage (2 kV) and $3\sigma_v$ equals to 1% of the amplitude of the primary current (22 A). A three-order digital Butterworth low-pass filter with a cutoff frequency of 25 Hz is applied to enhance the robustness of the online diagnostics method.

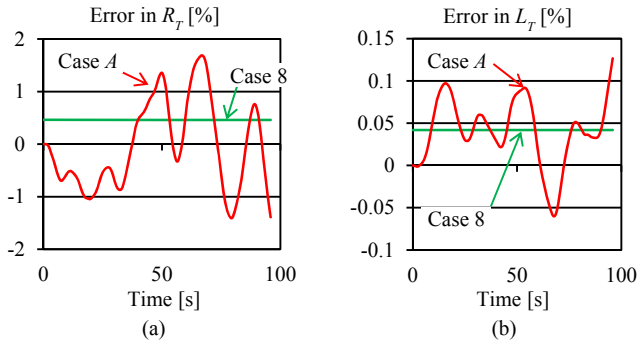

Fig. 7. Identification error considering 1% measurement noise; (a) Error in winding resistance R_T; (b) Error in leakage inductance L_T.

According to the simulation results shown in Fig. 7, the identification results are polluted by the measurement noise. For 1% noise on all voltages and currents, the maximum difference of the total leakage inductance is 0.13% and the maximum difference of the total winding resistance is 1.5%. The accuracy of the proposed diagnostics process is weakened, when the amplitude of the noise increases. For 3% noise level (6 kV and 66 A) on the measurements, the largest identification errors are 5% for the resistance and 0.5% for the inductance. Even with heavily polluted measurements, the accuracy of the leakage inductance is still acceptable. However, the error on the winding resistance is too large. This is so because the resistance is usually much smaller when compared with the leakage reactance of the transformer as mentioned in Section III.A. However sometimes it is possible that only a change of winding resistance can be observed (i.e. tap-changer contact oxidation). Hence, we still analyze the changes of winding resistance in the rest of the paper.

One way to enhance the accuracy is to increase the order of the low pass filter and reduce its cutoff frequency. With a five-order low-pass filter with 5 Hz cutoff frequency, the identification error on the winding resistance can be reduced to 3.03% with 3% noise. However, increasing the order and reducing the cutoff frequency of the low-pass filter will impact the dynamic performance of the filter. An example can be found in the next subsection.

D. Deformation Diagnostics with Sinusoidal Input and Linear Load

Leakage impedance identification is only half of the diagnostics process. A suitable diagnostics system should have the ability to identify both normal leakages and abnormal leakages. In this example, the transformer deformations are simulated by changing its leakage impedance. As mentioned before, according to the IEEE standard [14], transformer deformations are defined as 3% change of the leakage inductance and 5% change of the winding resistance. Hence, to capture the winding deformation successfully, the proposed method should be sensitive enough to the leakage impedance changes.

Three simulations with 1% measurement noise are performed in this example. In the first two simulations, a three-order low-pass filter with 25 Hz cutoff frequency is applied. In case *B*, the winding resistance and leakage inductance are increased by 5% and 3%, respectively. The winding

resistance and inductance are reduced by 5% and 3% in case *C*. In the third simulation (case *D*), we first simulate the case using a five-order low-pass filter with 5 Hz cutoff frequency. The three simulation results are shown in Fig. 8.

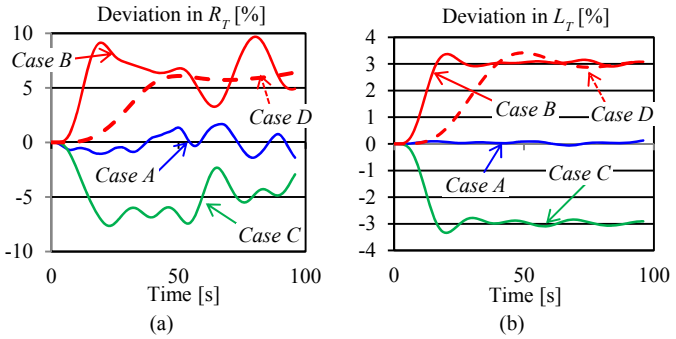

Fig. 8. Winding deformation diagnostics with linear load: (a) deviation of the winding resistance R_T; (b) deviation of leakage inductance L_T.

In all three simulations, the initial values of the low-pass filter are equal to the leakage impedance obtained from short-circuit test. Hence, explicit dynamic responses can be found in Figs. 8(a) and (b). It takes 20 s for the stabilization of the low-pass filter when winding deformations occur (the oscillations in Figs. 8(a) and (b) are created by the measurement noise). As mentioned before, if the order of the low-pass filter is increased and the cutoff frequency is reduced, the identification results become more robust to noise, but the stabilization time increases; see the dotted lines in Figs. 8(a) and (b).

After the output of the low-pass filter is stable, the deformations on both resistance and inductance can be found in Fig. 8. Although the identification results on the winding resistance are heavily polluted by measurement noise, one still can find resistive deformation looking at Fig. 8(a). In comparison, the proposed method is very accurate for inductive deformation detection. Since inductive deformation is the major deformation that occurs in practice, the proposed method can effectively detect incipient winding deformations.

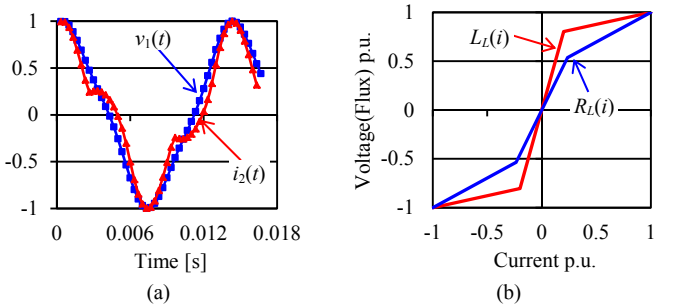

Fig. 9. (a) Normalized measurements of v_1 and i_2 for case E, the base voltage is 306.6 kV and the base current is 1.897 kA; (b) Normalized nonlinear behavior of the load resistor and inductor; the base voltage and current of the resistor are 280 kV and 1.698 kA, the base flux and current of the inductor are 747 Wb and 0.5 kA.

E. Distorted Input Voltage with Linear and Nonlinear Loads

In the previous study cases, we assumed that the input voltage is a sinusoidal function and the load fed by the transformer is linear. However, these two assumptions may not be correct in practice. Different from previous online diagnostics methods, the proposed method in this paper has no requirements of voltage quality or linear load behavior. Two numerical examples are provided next to validate this statement.

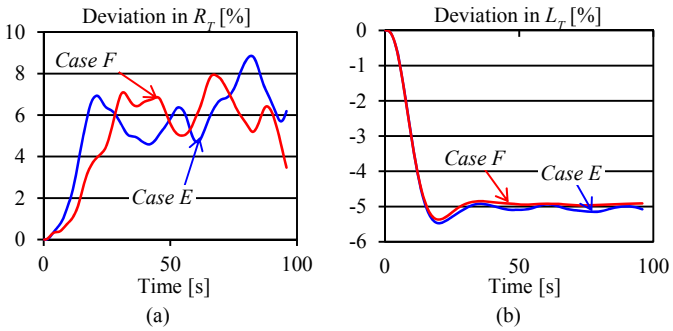

Fig. 10. Winding deformation diagnostics with non-sinusoidal excitation and nonlinear load: (a) deviation of the winding resistance R_T; (b) deviation of leakage inductance L_T.

The input voltage of the transformer is a combination of fundamental frequency and 3rd harmonic. The mathematical description of the voltage source is:

$$v(t) = V_m \cos(\omega t) + 0.1V_m \cos\left(3\omega t + \frac{\pi}{6}\right) \qquad (17)$$

The amplitude of the 3rd harmonic is set to be 10% of the fundamental frequency to produce an extremely bad input voltage. Two cases are simulated in this section. In the first case (case *E*), the transformer carries half load with a 0.707 leading power factor. The second case (case *F*) has the transformer connected to a nonlinear resistor and nonlinear inductor. The normalized primary terminal voltage and secondary current for case *E* are shown in Fig. 9(a). The normalized nonlinear behavior of the resistor and inductor are shown in Fig. 9(b). Similar to the previous studies, a 1% noise is added to the measurements in both simulation studies. The winding resistance is increased by 5% and the leakage inductance is reduced by 5% to create a different example. The results can be found in Fig. 10. One can observe that both resistive and inductive deformations can be detected under very severe circumstances (including input voltage harmonics, nonlinear loads, and noise). Although errors can be found in the identification results, the diagnosis results are still trustable.

IV. Validation by Finite Element Simulations and Lab Experiments

A. Finite Element Simulations

In the previous section, *T* equivalent and π equivalent circuits were used to generate the voltage and current measurements of a transformer with deformations. In this section, a Finite Element Model (FEM) of a 167 kVA commercial transformer is built in Ansoft Maxwell environment to simulate the voltage and current measurements; see Fig. 11(a).

The geometrical assumptions of the transformer model are discussed next. Both primary and secondary windings and the core are assumed to be solid bodies. The winding resistance measured at 60 Hz (taken from the datasheet) was used. All tests mentioned in this paper are done at 60 Hz. The sur-

rounding domain is padded to about 3 times in all the directions to ensure that all the flux remains inside the solution domain. We verified that a negligible error is introduced by the termination of the domain. A Neumann boundary condition is used as the external boundary. A magnetostatic analysis was carried out to determine the sensitivity of magnetizing and leakage inductance (calculated using the magnetic energy method) changing mesh size. Based on this analysis, appropriate mesh setting (70,831 elements) was chosen and used for the time-domain simulations. The online measurements are obtained from the voltmeter and ammeter available in the circuit interface of Ansys Maxwell. A cosine excitation is used in the circuit interface to avoid transformer inrush transients. The simulation time is 0.1 s and the time step is 1/3000 s.

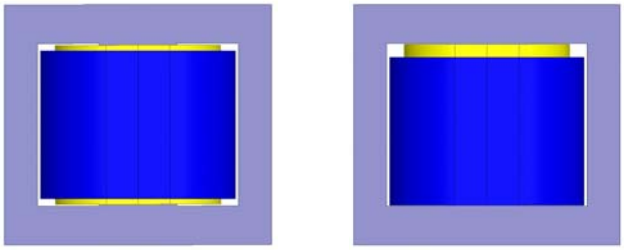

(a) (b)

Fig. 11. FEM of a 167 kVA transformer; (a) transformer model with no deformation; (b) transformer model with deformation (the winding has moved down 4 in).

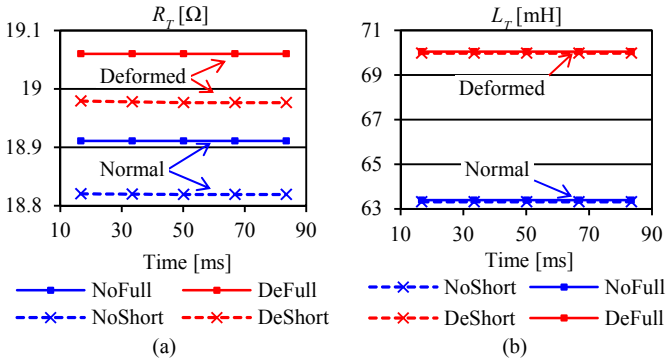

(a) (b)

Fig. 12. Winding deformation diagnostics of the finite element model; NoFull stands for transformer without deformation at full load, DeFull stands for deformed transformer at full load, NoShort stands for transformer with no deformation under short-circuit test, DeShort stands for deformed transformer under short-circuit test. (a) Winding resistance R_T; (b) Leakage inductance L_T.

The dimensions of the transformer and test results were obtained from a transformer manufacturer. The electrical parameters obtained with FEM simulations were validated with the data sheet of the transformer originally obtained experimentally.

Due to the electromagnetic forces on the low voltage windings, perhaps caused by an external short-circuit, the winding has fallen 0.4 in; see Fig. 11(b). We assume that the deformed and not deformed transformers are working at full load. The results of implementing the proposed online diagnostics method are shown in Fig. 12.

The results are compared with the short circuit tests for both deformed and not deformed transformers. According to Fig. 12(a), the maximum difference of the winding resistance is 1.3% which will not create a resistive deformation alarm. In contrast, a large difference (9.4%) on the leakage inductance can be found in Fig. 12(b). As a result, the inductive deformation alarm is created to inform the operator.

B. *Experimental Validation*

The proposed method has been validated with a lab experiment. The secondary of a small transformer (see Fig. 13) has been moved down to almost touch the yoke to create a winding deformation. The primary voltage and current recorded with a LabVIEW data acquisition module are shown in Fig. 14(a). The sampling frequency is 2.5 kHz. One can see from Fig. 14(a) that the primary voltage and current are not perfect sinusoidal waveforms. Fig. 14(b) presents the detection results without the use of a low-pass filter. As shown in Fig. 14(b), the proposed method can identify the transformer winding deformation when the transformer is loaded. The leakage inductance of the transformer has increased 18% when the secondary winding falls down. One can see that the differences between the calculated inductances (Lissajous method) and the standard short-circuit test results are negligible. With the help of a low-pass filter, the impact of the measurement noise can be eliminated; see Fig. 15.

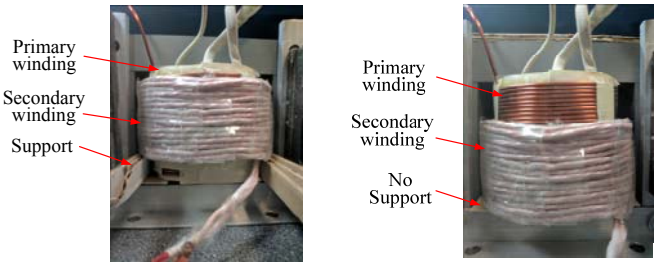

(a) (b)

Fig. 13. Experimental setup for winding deformation diagnostics system test; (a) normal transformer; (b) deformed transformer.

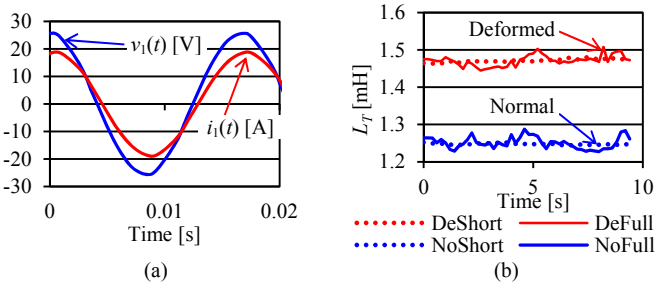

(a) (b)

Fig. 14. (a) Primary voltage and current; (b) Winding deformation diagnostics of leakage inductance L_T.

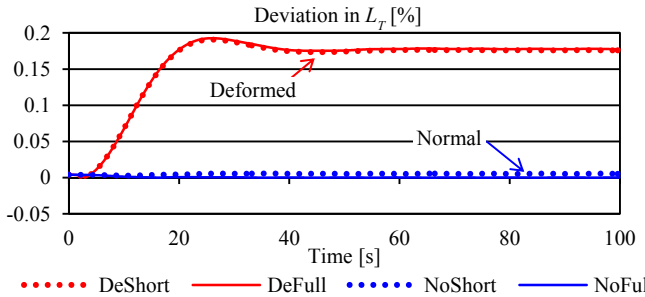

Fig. 15. Deviation of leakage inductance L_T obtained from winding deformation diagnostics results.

V. Conclusion

In this paper, a data-driven online diagnostics method for the detection of transformer winding deformation has been proposed. The method is robust even under extremely severe working conditions such as: noisy measurements, load changes, input harmonics, and system nonlinearities.

Several numerical examples illustrate the virtues of the proposed method. FEM simulations and a lab experiment confirm that the method can successfully detect the change of short-circuit impedance created by winding deformations. The results provided in this paper demonstrate that the novel method is implementable in practice for detecting transformer winding abnormality. Only information already available to the differential protection relay is needed. According to the case studies from cases D to E, the proposed method is more noise resistive for identifying the change in the leakage inductance which is usually caused by winding deformation. Hence, the proposed method is a promising candidate for detecting winding deformations.

Reference

[1] N. Hashemnia, A. A-Siada, and S. Islam, "Improved power transformer winding fault detection using FRA diagnostics – part 2: radial deformation simulation," *IEEE Trans. Dielectr. Electr. Insul.,* vol. 22, no. 1, pp. 564-570, May. 2014.

[2] M. Bagheri, M. S. Naderi, T. Blackburn, and B. T. Phung, "Frequency response analysis and short circuit impedance measurement in detection of winding deformation within power transformers," *IEEE Electr. Insul Mag.,* vol. 29, no. 3, pp. 33-40, 2013.

[3] L. M. Burrage, E. F. Veverka, and B. W. McConnell, "Steep front short duration low voltage impulse performance of distribution transformer," *IEEE Trans. Power Delivery*, vol. 2, no. 4, pp. 1152-1156, Oct. 1987.

[4] M. Bagheri, M. S. Naderi, and T. Blackburn, "Advanced transformer winding deformation diagnosis: moving from off-line to on-line," *IEEE Trans. Dielectr. Electr. Insul*., vol. 19, no. 6, pp. 1860-1870, Dec. 2012

[5] S. A. Ryder, "Diagnosing transformer faults using frequency responding analysis," *IEEE Electrical Insulation Magazine*, 2003, vol. 2, no. 19, pp. 16-22.

[6] J. C. Gonzales and E. E. Mombello, "Fault interpretation algorithm using frequency-response analysis of power transformers," *IEEE Trans. Power Delivery*, vol. 31, no. 3, pp. 1034-1042, Jun. 2016.

[7] M. Bagheri, M. S. Naderi, T. Blackburn, and T. Phung, "FRA vs. short circuit impedance measurement in detection of mechanical defects within large power transformer," *2012 IEEE International Symposium on Electrical Insulation*, San Juan, PR., pp. 301-305. Jul. 2012.

[8] V. Behjat, A. Vahedi, A. Setayeshmehr, H. Borsi, and E. Gockenbach, "Diagnosing shorted turns on the windings of power transformers based upon online FRA using capacitive and inductive couplings," *IEEE Trans. Power Del*., vol. 26, no. 4, Oct. 2011.

[9] T. D. Rybel, A. Singh, J. A. Vandermaar, M. Wang, J. R. Marti, and K. D. Srivastava, "Apparatus for online power transformer winding monitoring using bushing tap injection," *IEEE Trans. Power Del*., vol. 24, no. 3, pp. 996-1003, Jul. 2009.

[10] A. Abu-Siada and S. Islam, "A novel online technique to detect power transformer winding faults," *IEEE Trans. Power Del*., vol. 27, no. 2, pp. 849-857, Apr. 2013.

[11] A. Masoum, N. Hashemnia, A. A. Siada, M. Masoum, and S. Islam, "Online transformer internal fault detection based on instantaneous voltage and current measurements considering impact of harmonics," Accept for publishing by *IEEE Trans. Power Del*., available online.

[12] T. Hong and F. de León, "Lissajous curve methods for the identification of nonlinear circuits: calculation of a physical consistent reactive power," *IEEE Trans. Circuits and Syst. I: Regular Papers*, vol. 62, no. 12, pp. 2874-2885, Dec. 2015

[13] C. R. Vogel, *Computational Methods for Inverse Problems*, 2002, SIAM.

[14] IEEE Guide for Diagnostic Field Testing of Electric Power Apparatus-Part 1: Oil Filled Power Transformer, Regulators, and Reactors, IEEE Standard 62-1995 (R2005), Mar. 2005.

[15] F. Bengt, "Generation of finite difference formulas on arbitrarily spaced grids," *Mathematics of Computation*, vol. 51, no. 184, pp. 699-706, Oct. 1988.

[16] A. V. Oppenheim and R. W. Schafer, *Digital Signal Processing*. Englewood Cliffs, NJ: Prentice-Hall, 1975.

[17] F. de León, A. Farazmand, and P. Joseph, "Comparing the T and π equivalent circuits for the calculation of transformer inrush currents," *IEEE Trans. Power Del*., vol. 27, no. 4, pp. 2390-2398, Oct. 2012.

[18] DCG-EMTP (Development coordination group of EMTP) Version EMTP-RV, Electromagnetic Transients Program. [Online]. Available: http://www.emtp.com.

[19] X. Chen, "Negative inductance and numerical instability of the saturable transformer component in EMTP," *IEEE Trans. Power Del*., vol. 15, no. 4, pp. 1199-1204, Oct. 2000.

[20] Data Sheet of SEL-2414 Transformer Monitor, "SEL-2414 Transformer Monitor," Sept. 2016. [Online]. Available: http://selinc.com/products/2414.

[21] Manuals of T60 Transformer Management Relay, "T60 Instruction Manual for 7.3x product version (Rev. AB2)," Sept. 2015 [Online]. Available: http://www.gegridsolutions.com/multilin/catalog/t60.htm.

[22] M. Lambert, M. Martinez-Duro, Jean Mahseredjian, F. de León, F. Sirois, "Transformer leakage flux models for electromagnetic transients: critical review and validation of a new model," *IEEE Trans. Power Del*., vol. 29, no. 5, pp. 2180-2188, Oct. 2014.

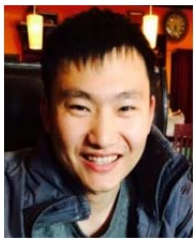

Tianqi Hong (S'13) was born in Nanjing, China, in 1989. He received the B.Sc. degree in electrical engineering from Hohai University, China, in 2011, and the M.Sc. degree in the electrical engineering from the Southeast University, China and the Engineering school of NYU in 2013. He received the Ph.D. degree from New York University in 2016.

He is currently a Postdoc Fellow in the Engineering School of NYU. His main interests are power system analysis, micro-grids, and electromagnetic field design.

Digvijay Deswal (S'16) completed his B. Tech. and M. Tech. degrees in Electrical Engineering at the Indian Institute of Technology (IIT) Kharagpur, West Bengal, India in 2014. He is currently a PhD candidate at New York University School of Engineering. His research interests include machine design, power electronics, and analysis of electrical machines.

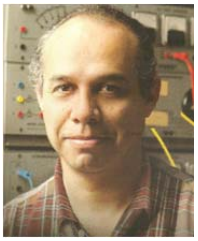

Francisco de León (S'86–M'92–SM'02–F'15) received the B.Sc. and the M.Sc. (Hons.) degrees in electrical engineering from the National Polytechnic Institute, Mexico City, Mexico, in 1983 and 1986, respectively, and the Ph.D. degree in electrical engineering from the University of Toronto, Toronto, ON, Canada, in 1992.

He has held several academic positions in Mexico and has worked for the Canadian electric industry. Currently, he is an Associate Professor with the Department of Electrical and Computer Engineering at New York University. His research interests include the analysis of power phenomena under non-sinusoidal conditions, the transient and steady state analyses of power systems, the thermal rating of cables and transformers, and the calculation of electromagnetic fields applied to machine design and modeling.

Prof. de León is an Editor of the IEEE Transactions on Power Delivery and the IEEE Power Engineering Letters.